START-TO-END SIMULATIONS FOR THE PROPOSED FERMILAB HIGH INTENSITY PROTON SOURCE *

J.-P. Carneiro†, D. Johnson‡, R.C. Webber
FNAL, Batavia, IL 60510, USA

Abstract

A High Intensity Proton Source consisting in an 8 GeV superconducting H-minus linac and transfer line to the Main Injector has been proposed. The primary mission is to increase the intensity of the Fermilab Main Injector for the production of neutrino superbeams. Start-to-end simulations from the RFQ to the stripping foil using the simulation code TRACK (ANL) is presented in this paper. In particular, we will study the impact of jitter errors on the H-minus phase space at the stripping foil.

INTRODUCTION

The FNAL superconducting H-minus linac is made of two major parts : an accelerating section and a transport line. The beam dynamics simulation codes TRACK [1] and MAD [2] are the main tools used for the design of the accelerating section and the transport line respectively. We have translated the MAD lattice of the transport line into TRACK format in order to perform start-to-end simulations of the complete accelerator (∼1.6 km). In particular, we study with this code the impact of jitter errors on the transverse and longitudinal beam parameters.

ACCELERATOR LAYOUT

Accelerating section

A layout of the accelerating section is presented in Figure 1 :

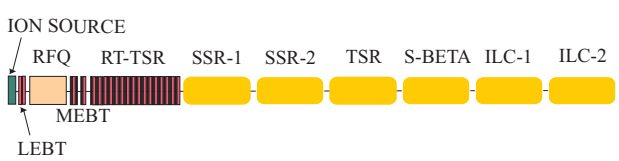

Figure 1: Layout of the accelerating section.

The main elements of the accelerating section (see Figure 1) are an H^- Ion Source, a Low Energy Beam Transport (LEBT) to match the beam into a Radio-Frequency Quadrupole (RFQ), a Medium Energy Beam Transport (MEBT) with 2 Room Temperature (RT) bunching cavities and a beam chopper followed by 16 RT Triple Spoke Resonators (RT-TSR), 18 superconducting Single Spoke Resonators of Type 1 (SSR1) and 33 longer ones (SSR2), 42 superconducting Triple Spoke Resonators (TSR), 56 Squeezed ILC-type superconducting cavities (S-ILC) designed for $\beta_G = 0.81$ followed by an ILC type section. The ILC-type section is divided in its first part (ILC-1) by 9 cryomodules containing each 7 ILC cavities and 2 quadrupoles. Two options are under study concerning the second part (ILC-2) : the first option [3] [4] consists in 28 cryomodules with 1 quadrupole and 8 ILC cavities per cryomodule while the second option makes use of 8 ILC RF units. We define in this paper [5] an ILC RF unit as containing 3 cryomodules each with 9 ILC cavities in the first and third cryomodule and 8 ILC cavities with one quadrupole in the second cryomodule. The focusing period is ∼3 times longer in this second option compared to the first one.

Transport line

The beam is transfered from the accelerating section to the MI-10 location in the Fermilab Main Injector by a ∼1 km transport line as presented in Figure 2:

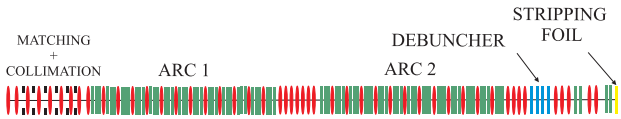

Figure 2: Layout of the transport line.

The transport line is a regular FODO lattice (60^0 phase advance per cell) made of two opposite signs arcs of 36 dipoles each. The dipoles are ∼6 meter long. As presented in Figure 2, 6 collimators are located in the matching section upstream the first arc and 4 debunchers cavities (necessary to reduce the momentum spread) downstream the second arc. The debuncher cavities are 17 cell superstructures operating at room temperature. Downstream the debuncher, the beam enters a matching section to get the desired beta functions at the stripping foil.

Parameters at the stripping foil

Figure 3 presents TRACK simulations of the horizontal beta function along the accelerator for a 45 mA beam current and the two options above-mentioned. Simulations included 3D space charge ($2 \cdot 10^5$ macro-particles) in the accelerating section and an ideal lattice (no alignment errors or jitters). The longer focusing period in the second option leads to a larger beta function for the 8 ILC units.

* Work supported by Fermi National Accelerator Laboratory operated by Fermi Research Alliance, LLC under Contract No. DE-AC02-07CH11359 with the United States Department of Energy.

† carneiro@fnal.gov
‡ dej@fnal.gov

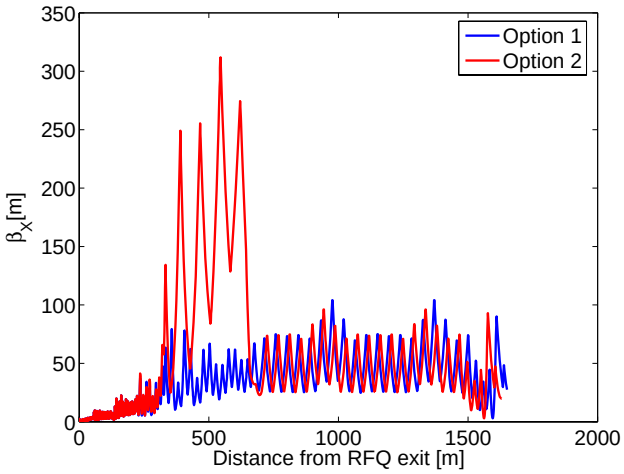

Figure 3: Horizontal beta function for the two options of the accelerator. Beam average current of 45 mA.

As shown in Table 1, both options present similar longitudinal and vertical beam parameters at the stripping foil at the exception of the transverse emittance. In fact, a transverse emittance dilution (∼40%) occurs in the second option compared to the first one. This is due to the weak focusing in the ILC units.

Table 1: Beam parameters at the stripping foil for both options of the accelerator. Beam average current of 45 mA.

Beam parameters	**Option 1**	**Option 2**
W [MeV]	8026	8006
σ_E [keV]	401	320
σ_Z [mm]	2.33	2.34
ϵ_Z [keV-mm]	869	725
σ_X / σ_Y [mm]	1.15 / 1.21	1.14 / 1.25
ϵ_X / ϵ_Y [mm-mrad]	0.46 / 0.50	0.62 / 0.70

STATISTICAL ERROR SIMULATIONS

This section presents the impact of RF errors and magnetic field errors on the beam dynamics for the lattice of the accelerator including the 8 ILC units (Option 2 abovementioned). The simulations were performed with TRACK on the Jazz cluster at ANL [6]. Three set of RF errors are considered : (0.5%, 0.5^0), (1%, 1^0) and (2%, 2^0) with for each set a magnetic field error (solenoids and quadrupoles) of $1 \cdot 10^{-3}$. The RF error distributions are Gaussian truncated at ± 3 rms value and the magnetic field errors are uniform with extreme values $\pm$ max. As for the "ideal" case discussed in the previous section (no errors), a beam current of 45 mA was considered and 3D space charge were implemented into TRACK in the accelerating section. The simulations were repeated 24 times starting every time from a different seed for the random generator and with $2 \cdot 10^5$ macro-particles. The debuncher cavities were set to

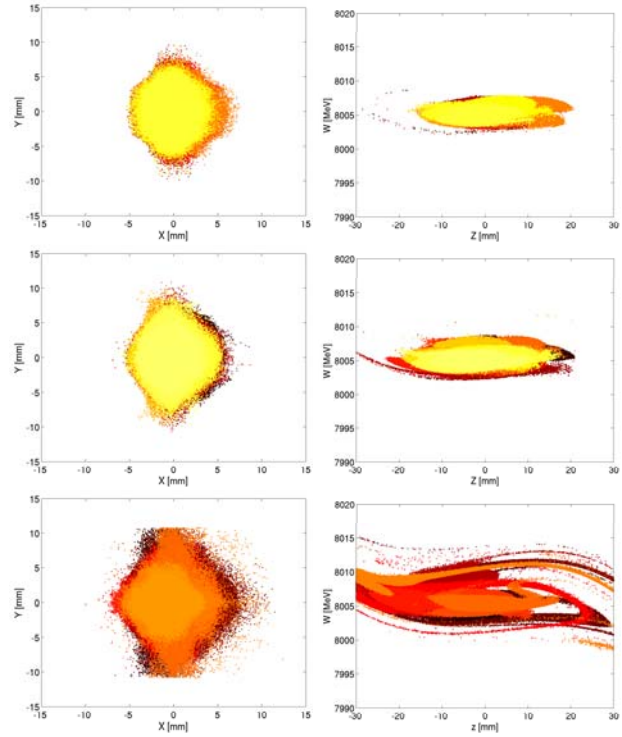

Figure 4: Transverse (left column) and longitudinal (right column) distributions at the stripping foil for 3 set of RF and magnetic field errors. First row : (0.5% 0.5^0 10^{-3}), second row : (1% 1^0 10^{-3}) and third row : (2% 2^0 10^{-3}).

minimize the energy spread and no collimators were used in the beamline. Figures 4 present the transverse and longitudinal beam distribution at the stripping foil with all the seeds superposed and Table 2 the corresponding statistical (mean and RMS deviation) beam parameters at the stripping foil.

Table 2: Beam parameters at the stripping foil for three sets of RF errors (magnetic field errors of $1 \cdot 10^{-3}$).

Beam param.	**0.5% 0.5^0**	**1% 1^0**	**2% 2^0**
W [GeV]	8006±0.5	8006±0.8	8006±1.6
σ_E [keV]	342±36	378±78	955±788
σ_Z [mm]	2.5±0.2	2.9±0.4	5.7±4.1
ϵ_Z [keV-mm]	827±81	998±182	5461±8046
σ_X [mm]	1.1±0.1	1.2±0.2	1.3±0.3
σ_Y [mm]	1.3±0.1	1.4±0.3	1.6±0.5
ϵ_X [mm-mrad]	0.6±0.1	0.6±0.1	0.9±0.3
ϵ_Y [mm-mrad]	0.7±0.1	0.7±0.1	1.0±0.3

We notice from Table 2 that RF and magnetic errors have a significant impact on the longitudinal parameters of the beam. It is interesting to notice that even with a set of errors of (2% 2^0 10^{-3}) we think the bunch length will fit within the MI RF bucket (53 MHz, ∼18.9 ns). In fact we want to inject into the central ±6 ns of the bucket (12 ns

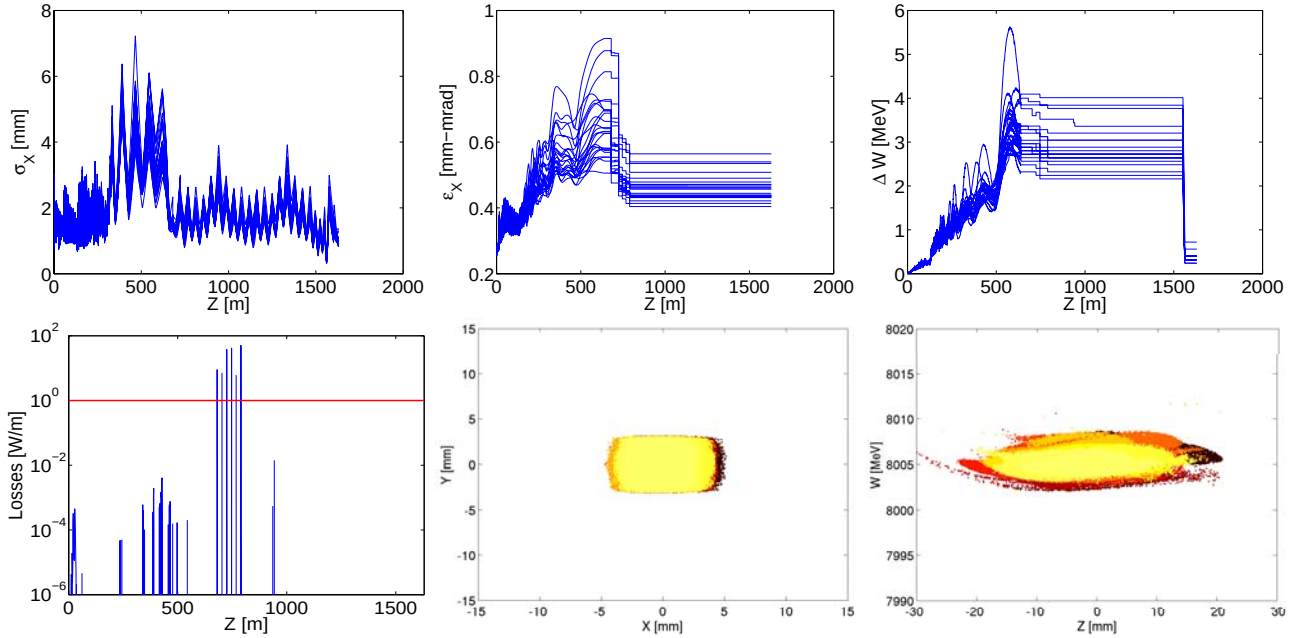

Figure 5: From top left to bottom right : RMS horizontal size, RMS horizontal normalized emittance, RMS energy spread, Beam losses, Transverse and Longitudinal distributions at the stripping foil. For a set of RF errors and magnetic field errors of (1% 1^0 10^{-3}) and a collimated beam of 45 mA.

total) which is about 4 linac RF buckets (325 MHz, ∼3 ns). With (2% 2^0 10^{-3}) the bunch length increases up to ∼150 mm which is only ∼0.5 ns and therefore should fit within a MI RF bucket. Concerning the stripping foil, temperature considerations have set a spot size of about 1.2 to 1.5 mm RMS on the foil which is within the range of the set (0.5% 0.5^0 10^{-3}) and (1% 1^0 10^{-3}). The set (2% 2^0 10^{-3}) would require significant collimation. From these simulations it looks like we would be comfortable with a set of RF and magnetic field errors of (1% 1^0 10^{-3}).

ERROR SIMULATIONS & COLLIMATION

Figure 5 shows TRACK simulations (24 seeds) for RF and magnetic errors of (1% 1^0 10^{-3}) with 6 collimators implemented between the accelerating section and the transport line (see Figure 2). The first 2 horizontal and vertical collimators have an half-aperture of 6 mm and the last ones of 5.5 mm. This configuration collimates ∼10% of the beam. Compared to the scenario (1% 1^0 10^{-3}) presented in previous section (no collimation), the horizontal normalized RMS emittance decreases by ∼20% (ϵ_x=0.46±0.04 mm-mrad) and the vertical by ∼40% (ϵ_y=0.42±0.04 mm-mrad), the horizontal RMS size of the beam at the stripping foil by ∼8% (σ_x=1.05±0.15) and the vertical by ∼30% (σ_x=0.95±0.15). Impact of the collimation is shown is Figure 5 with a decrease of the RMS horizontal normalized emittance and a square like shape transverse beam distribution at the stripping foil. As expected, we did not observe a significant impact of the transverse collimation on the longitudinal beam parameters.

CONCLUSION

Start-to-End simulations of the Fermilab High Intensity Proton Source have been presented in this paper. The simulations were performed with the code TRACK for an average beam current of 45 mA, with $2 \cdot 10^5$ macro-particles and 3D space charge effects in the accelerating section. Impact of three sets of RF errors (0.5% 0.5^0), (1% 1^0) (2% 2^0) was investigated with magnetic field errors of 10^{-3} and a lattice of the accelerator including 8 ILC RF units. From these simulations it looks like we would be comfortable with a set of RF and magnetic field errors of (1% 1^0 $1 \cdot 10^{-3}$)

ACKNOWLEDGMENT

The authors would like to thank P. Ostroumov (ANL) for many useful discussions, B. Mustapha (ANL) for his help on using TRACK and J. Valdes (ANL) for his assistance with Jazz. The authors also wish to thank V. Shiltsev for his support with this work.

REFERENCES

[1] V.N. Aseev, P.N. Ostroumov, E.S. Lessner and B. Mustapha, “TRACK : The new beam dynamics code”, PAC 2005.

[2] H. Grote, F. C. Iselin, The MAD Program, Version 8.10.

[3] G.W. Foster (Editor), Available at : http://protondriver.fnal.gov/SCRF_PD_v56.doc

[4] P.N. Ostroumov, “Physics design of the 8-GeV H-minus Linac” , New Journal of Physics, **8**, 281 (2006).

[5] A. Valishev, private communication.

[6] JAZZ wweb site : http://www.lcrc.anl.gov